ORIGINAL PAPER

BSA-PEI Nanoparticle Mediated Efficient Delivery of CRISPR/Cas9 into MDA-MB-231 Cells

Hossein Rahimi[1] · Kasra Arbabi Zaboli[1] · Jose Thekkiniath[2] · Seyed Hossein Mousavi[3] · Behrooz Johari[1,8] · Mohammad Reza Hashemi[4] · Hamed Nosrati[5] · David Goldschneider[6] · Agnes Bernet[7] · Hossein Danafar[5] · Saeed Kaboli[1,8]

Abstract

The discovery of bacterial-derived Clustered Regularly Interspaced Short Palindromic Repeats (CRISPR)/CRISPR-associated protein 9 (Cas9) system has revolutionized genome engineering and gene therapy due to its wide range of applications. One of the major challenging issues in CRISPR/Cas system is the lack of an efficient, safe, and clinically suitable delivery of the system's components into target cells. Here, we describe the development of polyethylenimine coated-bovine serum albumin nanoparticles (BSA-PEI NPs) for efficient delivery of CRISPR/Cas9 system in both DNA (px458 plasmid) and ribonucleoprotein (RNP) forms into MDA-MB-231 human breast cancer cell line. Our data showed that synthesized BSA-PEI (BP) NPs delivered plasmid px458 at concentrations of 0.15, 0.25, and 0.35 μg/μl with efficiencies of approximately 29.7, 54.8, and 84.1% into MDA-MB-231 cells, respectively. Our study demonstrated that Cas9/sgRNA RNP complex efficiently (~ 92.6%) delivered by BSA-PEI NPs into the same cells. Analysis of toxicity and biocompatibility of synthesized NPs on human red blood cells, MDA-MB-231 cells, and mice showed that the selected concentration (28 μg/μl) of BSA-PEI NPs for transfection had no remarkable toxicity effects. Thus, obtained results suggest BSA-PEI NPs as one of the most promising carrier for delivering CRISPR/Cas9 to target cells.

Keywords BSA-PEI · CRISPR/Cas9 · Nanoparticles · Delivery

Introduction

The discovery of bacterial-derived Clustered Regularly Interspaced Short Palindromic Repeats (CRISPR)/CRISPR-associated protein 9 (Cas9) system has revolutionized genome engineering and gene therapy due to its wide range of applications [1–5]. CRISPR (with its diverse Cas proteins) compared to previous genome engineering techniques such as Transcription Activator-Like Effector Nucleases (TALEN), Zinc-Finger Nucleases (ZFNs), and Meganucleases has superiorities including cheapness, high accuracy, specificity, easy design, potency, and versatility so that it has become a promising therapeutic and diagnostic option for many diseases. The CRISPR/Cas9 genome editing system consists of two key components, including Cas9 endonuclease and guide RNA (gRNA), which recognizes the target region through gRNA and makes cleavage in the target site using the Cas9 enzyme [6–9]. This system provides a simple to multiplex platform for the precise and specific modification and exploitation of organisms' genome in diverse fields, ranging from biotechnology research to therapeutics. Since this technology allows direct modification of disease-causing genes as well as the production of personalized anti-tumor immune cells, it is an ideal way to implement personalized treatment for different diseases particularly cancer [10, 11]. CRISPR/Cas systems are extensively employed to develop novel solutions for treating and diagnosing a wide range of diseases, notably infectious diseases (recently for COVID-19 diseases [12]). Its applications have been revolutionary in a variety of biological and therapeutic fields, and was awarded the Nobel Prize in Chemistry [5, 13]. The most challenging issues in therapeutic applications of genome editing tools especially the CRISPR/Cas9 system are the

✉ Hossein Danafar
danafar@zums.ac.ir

✉ Saeed Kaboli
kaboli2009@gmail.com

Extended author information available on the last page of the article

efficient, safe, and clinically appropriate gene delivery into target cells in vitro or in vivo [14–16]. In this regard, common delivery approaches generally include physical, viral, and non-viral delivery methods. Physical delivery methods, including electroporation and microinjection, allow direct delivery of CRISPR system components. However, these methods generally require specialized equipment that are not suitable for in vivo gene delivery as an ultimate delivery goal in the gene therapy [17, 18]. Viral vectors, despite their wide range of benefits and applications, face limitations including low loading capacity, induction of the immune response, and the risk of integration into the host genome [19–21]. Among non-viral delivery methods, the design and use of nanoparticles (NPs) as safe and efficient carriers for the delivery of CRISPR system's components has recently received special attention [22–25]. So far, various types of NPs including gold NPs, polymer NPs, lipid NPs, peptide NPs, and DNA nanostructures have been employed to deliver the CRISPR/Cas9 system. In general, in CRISPR designs, NPs have outstanding advantages such as easy synthesis, high loading capacity, in vitro and in vivo applicability, low cost, and high efficiency [26–33]. In this study, Bovine Serum Albumin (BSA) coated with polyethylenimine (PEI) was used to deliver CRISPR/Cas9 system in plasmid and ribonucleoprotein (RNP) forms into the MDA-MB-231 cells; as in this structure PEI binds to the surface of BSA through electrostatic interactions. PEI coating was used with the aim of increasing cellular uptake by positively charging NPs surface as well as facilitating endosomal escape for successful delivery [34–37]. When PEI-coated NPs enter the cell through endocytosis mechanism, the protonation of amines leads to influx of positively charged ions, and thus the osmotic potential is reduced. Osmotic swelling may lead to endosome instability and the BSA-Cas9/sgRNA-PEI NPs are released into the cytoplasm [38, 39]. As albumin protein is one of the most essential proteins in human and animals it may be employed as an appealing delivery option because it originates from a natural source and does not have toxicity and immunogenicity. In the present study, we aimed to evaluate the efficacy of BSA-based NPs in successful, safe, and effective delivery of CRISPR/Cas9 system components on cancer cell line. For this purpose, we generated plasmid (px458) and RNP forms of the system and delivered in MDA-MB-231 cells separately. To our knowledge, this is the first study that reports on BSA-based NPs mediated delivery of CRISPR/Cas9 components in MDA-MB-231 cell.

Methods

Synthesis of BSA-PEI Nanoparticles

For the synthesis of BSA NPs, 45 mg of BSA powder (Sigma-Aldrich) was dissolved in PBS buffer and then an ethanolic solution of PEI (MW ~ 1800) (Sigma-Aldrich) was added to BSA solution. PEI coating packages the BSA NPs and is considered to escape from endosomes (Fig. 1). PEI ethanolic solution forms only a very small ratio of the total reaction volume (0.4%). The two fundamental constituents of the formulation, BSA and PEI, were used in a ratio of approximately 45:1 (45 mg of BSA and 1.071 mg of PEI).

Determination of Zeta Potential and Diameter of NPs

Dynamic light scattering (DLS; Malvern Instruments, Worcestershire, UK, model Nano ZS) was used to determine the size of the synthesized BSA-PEI (BP) NPs. Also, nano/zeta sizer (Malvern Instruments Ltd.) was used to determine the surface charge of the BSA-PEI NPs.

TEM

Transmission electron microscopy (TEM, Cambridge 360–1990 Stereo Scan Instrument-EDS, CA) was used to determine the size and morphology of the synthesized NPs.

Hemolysis Assay

Hemolysis assay using human blood was used to evaluate the blood compatibility of the designed NPs. To separate the red blood cells, the blood sample was centrifuged at 3000 rpm for 10 min, and the resulting precipitated red blood cells were washed several times with PBS until the supernatant liquid becomes transparent and 100 µl of washed red blood cells were used for hemolysis.

Various concentrations of NPs (140, 224, and 280 µg/µl) were added to red blood cells with 1 ml PBS. Deionized water was used as a positive control, and PBS was used as a negative control. The samples were shaken at 37 °C in a shaker incubator. The samples were centrifuged at 13,000 rpm for 15 min and the absorbance of supernatant was read at 540 nm. The percentage of hemolysis was calculated by the following formula:

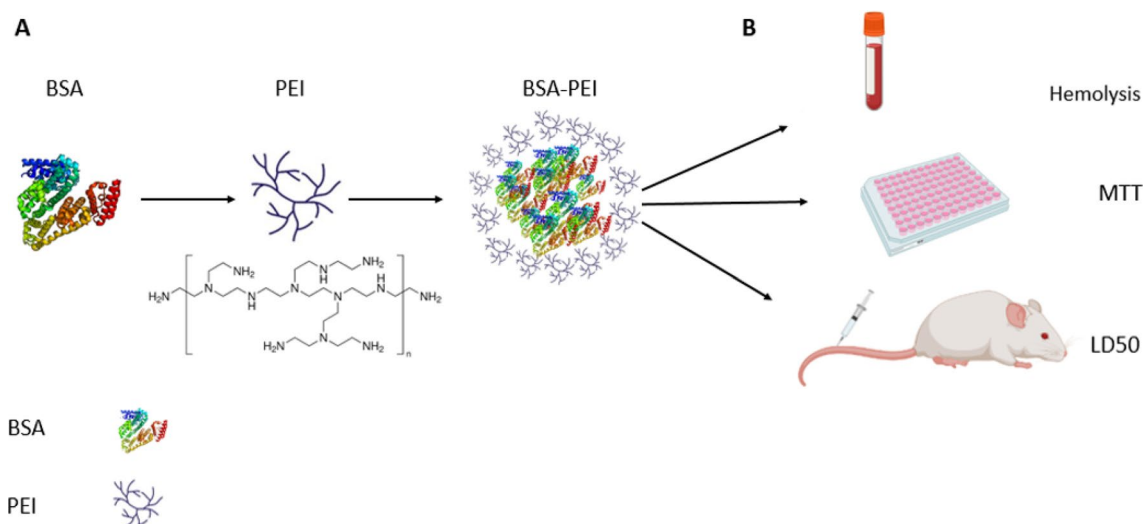$$Hemolysis\ (\%) = \frac{A\ sample - A\ negative}{A\ positive - A\ negative} \times 100$$

Fig. 1 A schematic illustration of synthesis and biological compatibility assays of BSA-PEI NPs. Preparation of BSA-PEI NPs (**A**) The biological compatibility of synthesized BSA-PEI NPs was evaluated by hemolysis, MTT, and LD_{50} assays (**B**)

Construction of BSA-px458 Plasmid-PEI Complex

To load px458 plasmid (pSpCas9 (BB)-2A-GFP; Addgene #48,138) on nanoparticles, BSA powder was dissolved in PBS buffer, and px458 plasmid at various concentrations (0.15, 0.25, and 0.35 μg/μl) was added to BSA solution, and mixed for 5 min. Finally, PEI was added to reaction and vortexed for 5 min (Fig. 2).

SgRNA In Vitro Transcription

Since we aimed to construct the sgRNA/Cas9 RNP complex for delivery by BSA-PEI NPs, synthesis of the sgRNA transcript (mRNA) from sgRNA (contains targeting sequence for the coding region of the CD81 gene [40]) ligated px458 plasmid is required. To this end, GeneArt™ Precision gRNA Synthesis Kit (Thermo Fisher Scientific) was used to synthesize sgRNA transcript from the cloned px458 plasmid. Forward and reverse primers were designed to amplify the cloned gRNA sequence in the px458 plasmid as well as the complete gRNA scaffold from the px458 plasmid. Since the T7 promoter is required to perform in vitro transcription, the T7 promoter sequence was added to the beginning of the forward primer when designing the primer. The designed primers are as follows:

Forward: 5'-TTAATACGACTCACTATAGGATGACGC CAACAACGCCA-3'.

Reverse: 5'-AAAAGCACCGACTCGGTGCC-3'.

Preparation of Cas9/sgRNA RNP Complex

To benefit from the RNP form of the CRISPR/Cas9 system in gene and cell therapy, the Cas9-GFP-NLS protein (abm, Canada) needs to be combined with the sgRNA to form the final Cas9/sgRNA RNP complex. To this end, the Cas9 protein was combined with the sgRNA in 1:1 ratio. Since the established Cas9/sgRNA RNP complex was to be examined in two modes (on extracted genomic DNA and inside of the cell), the Cas9/sgRNA RNP complex reaction was performed in two modes. First, for complexing the Cas9 and sgRNA to analyze the cleavage activity of the created Cas9/ sgRNA complex on the extracted genomic DNA, 0.35 μg/ μL Cas9 protein and 0.35 μg/μL sgRNA were combined in 3 μL Cas9 assembly buffer, and finally the created solution was added to 20 μL deionized water and incubated at 37 °C for 15 min. Second, for complexing the Cas9 protein and sgRNA to delivery into MDA-MB-231 cells, PBS was used as the reaction medium.

Construction of BSA-RNP-PEI Complex

To load the Cas9/sgRNA RNP complex on BSA-PEI nanoparticles, BSA powder was dissolved in PBS and after mixing, the RNP complex was added to the BSA solution, and vortexed for 5 min. Finally, PEI was added to the reaction and vortexed for 5 min (Fig. 3).

Cytotoxicity Assay

In this study, effects of BSA_{1-3} (28.0, 44.8 and 56 μg/ μl), BSA-PEI (BP_{1-3}: 28.0, 44.8 and 56 μg/μl), BSA-px458

Fig. 2 The schematic illustration of construction of BSA-px458 plasmid-PEI complex. BSA was dissolved in PBS and then plasmid was added to BSA solution and after vortexing the obtained solution, PEI was added to the BSA-plasmid solution resulting in BSA-px458 plasmid-PEI complex (**A**). Cellular internalization of the prepared BSA-px458 plasmid-PEI complex (**B**)
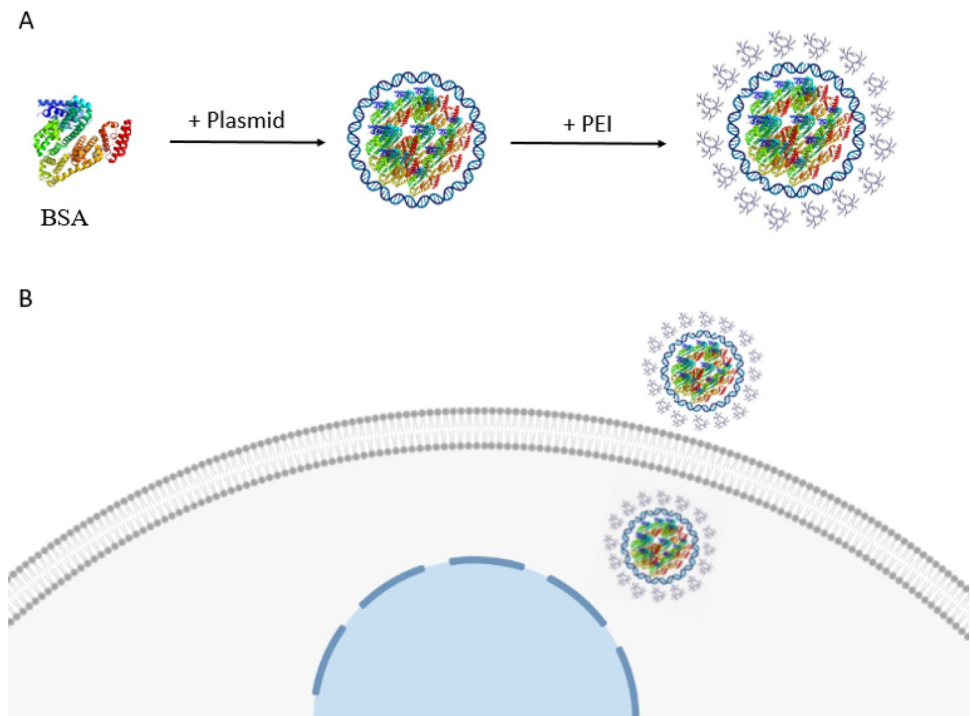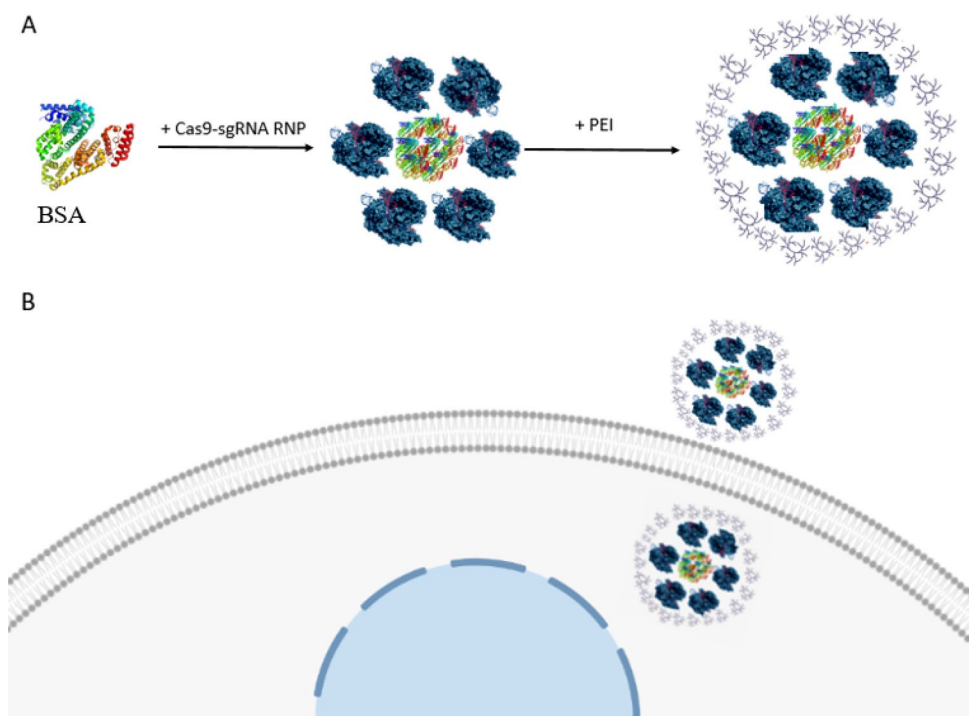

Fig. 3 A schematic diagram on construction of BSA-RNP-PEI complex. BSA was dissolved in PBS, RNP complex was added to BSA solution, and after mixing, PEI was added to the BSA-RNP solution resulted in BSA-RNP-PEI complex (**A**). Cellular internalization of prepared BSA-RNP-PEI complex (**B**)

plasmid-PEI (BP-P$_{1-3}$: 28.0, 44.8 and 56 µg/µl that each concentration mixed with 0.35 µg/µl of px458 plasmid), BSA-RNP-PEI (BP-RNP$_{1-3}$: 28.0, 44.8 and 56 µg/µl that each concentration mixed with 0.35 µg/µl of RNP), RNP (0.35 µg/µl), px458 plasmid (0.35 µg/µl) and DNA fectamine (DNAfec: 4 µl) on the survival of MDA-MB-231 cells were examined. MDA-MB-231 cells were seeded in a 96-well

plate at a standard density (1.5×10^4 cells per well) and incubated in 10% FBS-supplemented DMEM medium for 24 h. Afterward, the culture media were replaced with the optiMEM containing selected groups of synthesized NPs and NPs-CRISPR complexes and incubated for 24 h. Then, the treatment media were replaced with 20 µL of MTT reagent and incubated for 4 h. Finally, after removing MTT

Fig. 4 The diameter distribution of BSA-PEI NPs. The DLS results of synthesized particles revealed that the diameter distribution of BSA and BSA-PEI NPs were, respectively, 32 nm and 102.50 nm. The polydispersity index (PDI) of BSA and BSA-PEI NPs were 0.2 and 0.4, respectively
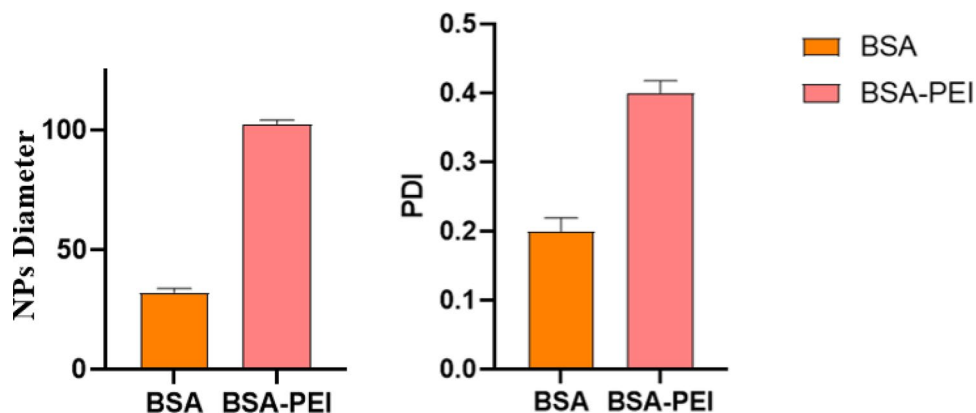
solution, formed formazan was dissolved in 150 μL of DMSO and then the absorbance of the wells was recorded by ELISA reader at 570 nm wavelength.

Delivery Efficiency Assay

To evaluate the delivery efficiency of BSA-RNP-PEI and BSA-px458 plasmid-PEI (carry GFP marker) into the MDA-MB-231 cells, 5×10^4 cells were cultured in each well of a 24-well plate, and incubated for 24 h (5% CO_2 and 37 °C). After 24 h of incubation, the culture media was aspirated and the cells were transfected with px458 plasmid at concentrations 0.15, 0.25, and 0.35 μg/μl and RNP (0.35 μg/μl) complexed with BSA-PEI NPs (28 μg/μl). The uptake of BSA-px458 plasmid-PEI and BSA-RNP-PEI complexes into cells were investigated by fluorescence microscopy and flow cytometry 72 h after transfection.

Determination of NPs Toxicity In Vivo

LD_{50} assay was used to evaluate the safety of the synthesized NPs in vivo. Different concentrations of BSA-PEI NPs including 39.50, 59.26, 88.88, 133.33, and 200 mg/kg were injected intravenously into BALB/c mice. Each concentration was injected into 4 mice to determine LD_{50}. Three parameters including mortality, body weight, and behavior of mice were monitored for 30 days.

Statistical Analysis

Graphpad Prism 9.0 (Graphpad software, San Diego, CA) and Microsoft excel (version 16.37) were used for statistical analysis. All values were presented as mean ± standard deviation (mean ± SD). Also, for multiple comparisons one-way analysis of variance (ANOVA) was used. P < 0.01(**) and P < 0.0001(****). All experiments were carried out in triplicates.

Results

Synthesis of BSA-PEI NPs

BSA-PEI NPs were synthesized using BSA and PEI (MW ~ 1800) to deliver CRISPR/Cas9 components in both plasmid and ribonucleoprotein forms into MDA-MB-231 cells. BSA was chosen in this study due to its unique properties including non-toxicity, non-immunogenicity, biodegradability, cheapness, availability, and easy synthesis [14]. PEI is a cationic polymer that compresses the Cas9/sgRNA-loaded BSA particles into a nanoscale complex that is efficiently absorbed by cells with the anionic surface by the endocytosis mechanism, which allows successful delivery. A previous study showed the use of a branched form of PEI (BPEI-25 kDa) as a carrier and evaluated for Cas9/sgRNA plasmid delivery. It was demonstrated that Cas9/sgRNA targeting of Slc26a4 locus efficiently delivered into Neuro2a cells by PEI [36].

Size Distribution and Zeta Potential

The size distribution and zeta potential of BSA-PEI NPs were determined by dynamic light scattering (DLS). As shown in Fig. 4, the average size of BSA and BSA-PEI NPs were approximately 32 nm (polydispersity index (PDI) = 0.2) and 102.50 nm (PDI = 0.4), respectively. Also, the surface charge of BSA and BSA-PEI NPs were about -14 mV and 3.1 mV, respectively.

The Morphology of BSA-PEI NPs

The BSA-PEI NPs morphology was analyzed by transmission electron microscopes (TEM). As illustrated in Fig. 5, the TEM image showed the spherical shape of the BSA-PEI nanoparticles, which confirms the correctness of the synthesis process.

Hemolysis Assay

Hemolysis assay is a method used to evaluate hemocompatibility of BSA-PEI NPs. In this assay, distilled water (dH$_2$O) and PBS were used as positive and negative controls,
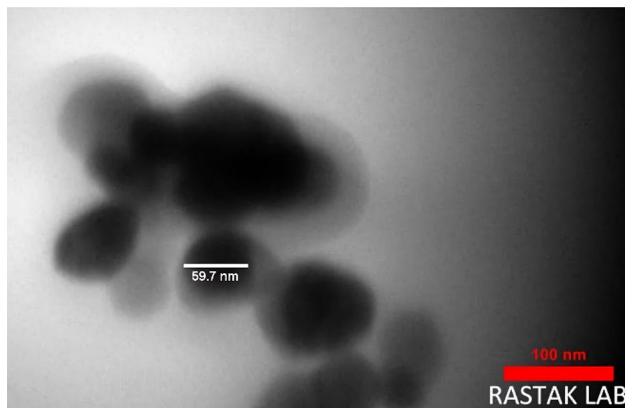

Fig. 5 TEM image of synthesized BSA-PEI NPs. The spherical shape of BSA-PEI NPs was observed by TEM, verifying the synthesis reaction
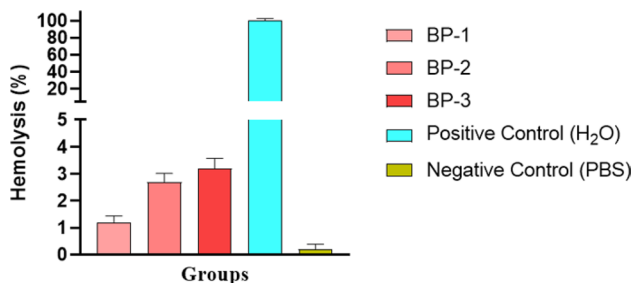

Fig. 6 Hemolysis activity of BSA-PEI NPs at various concentrations. The hemocompatibility concentrations of 140, 224, and 280 µg/µl of BSA-PEI NPs were examined, and the selected concentrations of BSA-PEI NPs showed appropriate hemolytic rate. (BP; BSA-PE, dH$_2$O; distilled water, PBS; phosphate-buffered saline)

respectively. This test was performed on BSA-PEI NPs with concentrations including 140, 224, and 280 µg/µl (fivefold concentrations used in the MTT assay). As shown in Fig. 6, selected concentrations of BSA-PEI (BP$_{1-3}$: 28.0, 44.8 and 56 µg/µl) showed suitable hemolytic rate including 1.2, 2.7, and 3.2%, respectively. Generally, a percentage of hemolysis less than 2% indicates that the sample is non-hemolytic. In addition, hemolysis rates of 2–5% and more than 5% indicate that the test sample is slightly hemolytic and hemolytic, respectively [41].

Cell Viability Evaluation

MTT assay was used to evaluate the effect of synthesized NPs on MDA-MB-231 cell's viability. Different concentrations of BSA, BSA-PEI, BSA-px458 plasmid-PEI, px458 plasmid, RNP, BSA-RNP-PEI, and DNA fectamine were investigated. Three concentrations of BSA$_{1-3}$ (28, 44.8, and 56 µg/µl) were evaluated to ensure that BSA was not toxic. As shown in Fig. 7, BSA had no toxic effect on MDA-MB-231 cells. The treated cells with all concentrations of the BSA-PEI (BP) NPs except 28 µg/µl indicated significant cell viability reduction compared to the control group. In addition, the cells treated with the BSA-px458 plasmid-PEI (BP-P$_{1-3}$) and BSA-RNP-PEI (BP-RNP$_{1-3}$) had significant cytotoxicity in comparison with the control group. When 28 µg/µl of the BSA-PEI NPs (BP$_1$) in complex with different concentrations of plasmid or RNP was used, cell viability was significantly reduced compared to BP$_1$ group. Therefore, concentration of 28 µg/µl was selected as the safe and optimal concentration of BSA-PEI for the delivery of CRISPR/Cas9 components.

Evaluation of Transfection Efficiency

To evaluate the CRISPR/Cas9 system's components delivery efficiency by BSA-PEI NPs, the cells were transfected with 0.15, 0.25, and 0.35 µg/µl px458 plasmid in complex
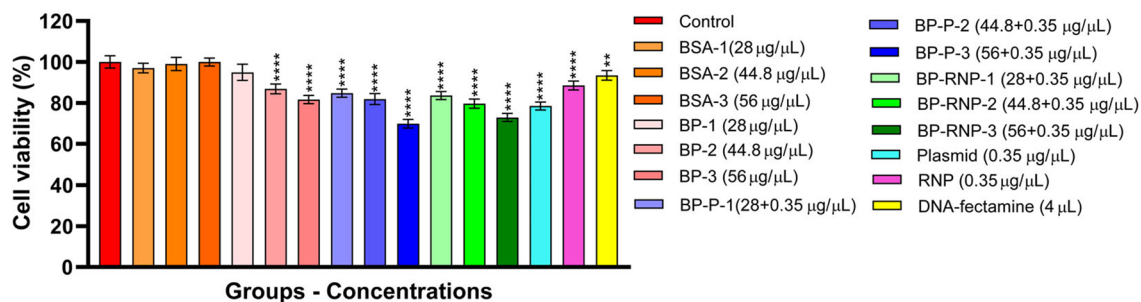

Fig. 7 The effect of different concentrations of BSA, BSA-PEI, BSA-px458 plasmid-PEI, BSA-RNP-PEI, px458 plasmid, RNP and DNA fectamine on viability of MDA-MB-231 cells. P < 0.01 (**) and P < 0.0001(****). BP; BSA-PEI, BP-P; BSA-PEI-Plasmid, BP-RNP; BSA-PEI-RNP
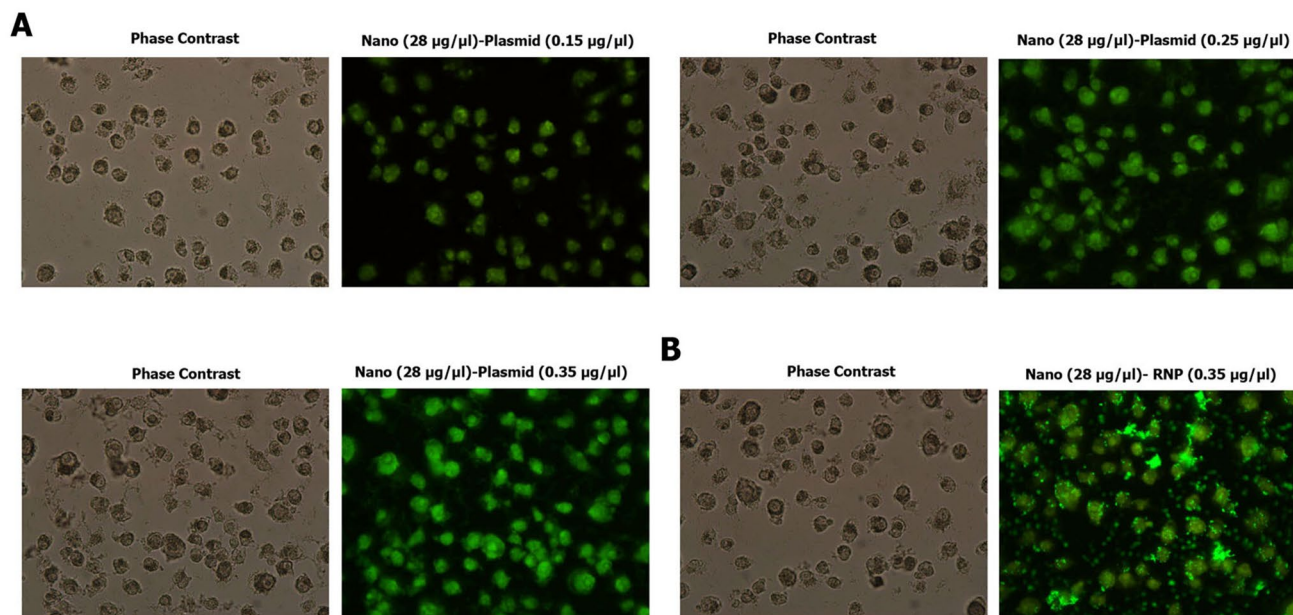
Fig. 8 The image illustration of delivery of px458 plasmid with concentrations of 0.15, 0.25, and 0.35 μg/μl (**A**), and RNP with concentration of 0.35 μg/μl (**B**) in complex with Nano (BP: 28 μg/μl) into MDA-MB-231 cells 72 h after transfection

with BSA-PEI NPs and also 0.35 μg/μl of RNP in complex with BSA-PEI NPs. Since the px458 plasmid and Cas9 protein harbor GFP marker, the fluorescence microscopy was used to evaluate whether the BSA-PEI nanoparticles could deliver the system's components into MDA-MB-231 cells. As shown in Fig. 8, the BSA-PEI NPs effectively delivered the px458 plasmid into high number of cells. Since the 3 selected concentrations of px458 plasmid are at low concentrations, successful delivery indicates high efficiency and high encapsulation efficiency of the designed nanoparticles. Also, as shown in Fig. 8, the BSA-RNP-PEI efficiently introduced into MDA-MB-231 cells. The highest delivery efficiency for BSA-px458 plasmid-PEI and BSA-RNP-PEI complexes was observed after 72 h of incubation. Also, the delivered BSA-px458 plasmid-PEI and BSA–RNP-PEI complexes stayed in the cells for a long period without affecting cell growth.

Flow Cytometry Analysis

The delivery efficiency of BSA-px458 plasmid-PEI and BSA-RNP-PEI complexes was analyzed by flow cytometry. As shown in Fig. 9A, B, flow cytometry analysis revealed that the BSA-PEI NPs delivered the concentrations of 0.15, 0.25, and 0.35 μg/μl plasmid px458 with an efficiency of 29.7 ± 2.8, 54.8 ± 1.5, and $84.1 \pm 1.3\%$ into MDA-MB-231 cells, respectively. Since we used low concentrations of px458 plasmid in delivery by BSA-PEI NPs as compared to similar studies, the efficiency up to 84.1% in the delivery of low concentrations of plasmid doubled

the value of BSA-PEI NPs. In addition, px458 plasmid in complex with NPs showed very low transfection efficiency indicating an important effect of BSA-PEI NPs in delivery. Moreover, flow cytometry analysis revealed that BSA-PEI NPs have an efficiency of $92.6 \pm 1.6\%$ in delivering RNP complex into MDA-MB-231 cells while the commercial agent, DNAfectamine showed 83.3% efficiency in RNP delivery (Fig. 9). The similarities of delivery efficiency of BSA-PEI NPs as compared to commercial agent (DNAfectamine) indicate a higher efficiency of BSA-PEI NPs in this study.

LD$_{50}$ Assay

The in vivo biosafety of synthesized NPs was investigated in healthy mice, since biocompatibility of nanoparticles is critical for in vivo applications. The in vivo biosafety evaluation of BSA-PEI NPs was performed in BALB/c mice following intravenous (IV) injection of selected concentrations (39.50, 59.26, 88.88, 133.33, and 200 mg/kg) of BSA-PEI NPs. The treated group of mice were monitored for 30 days and the mortality and body weight of mice were documented. As shown in Fig. 10, the LD$_{50}$ showed that the BSA-PEI NPs was safe up to 200 mg/kg. Also, the treated mice as compared to control group showed no death nor abnormal body weight changes (Fig. 10). Therefore, our results suggested that the BSA-PEI NPs have no adverse effects on in vivo condition in the range of selected concentrations.
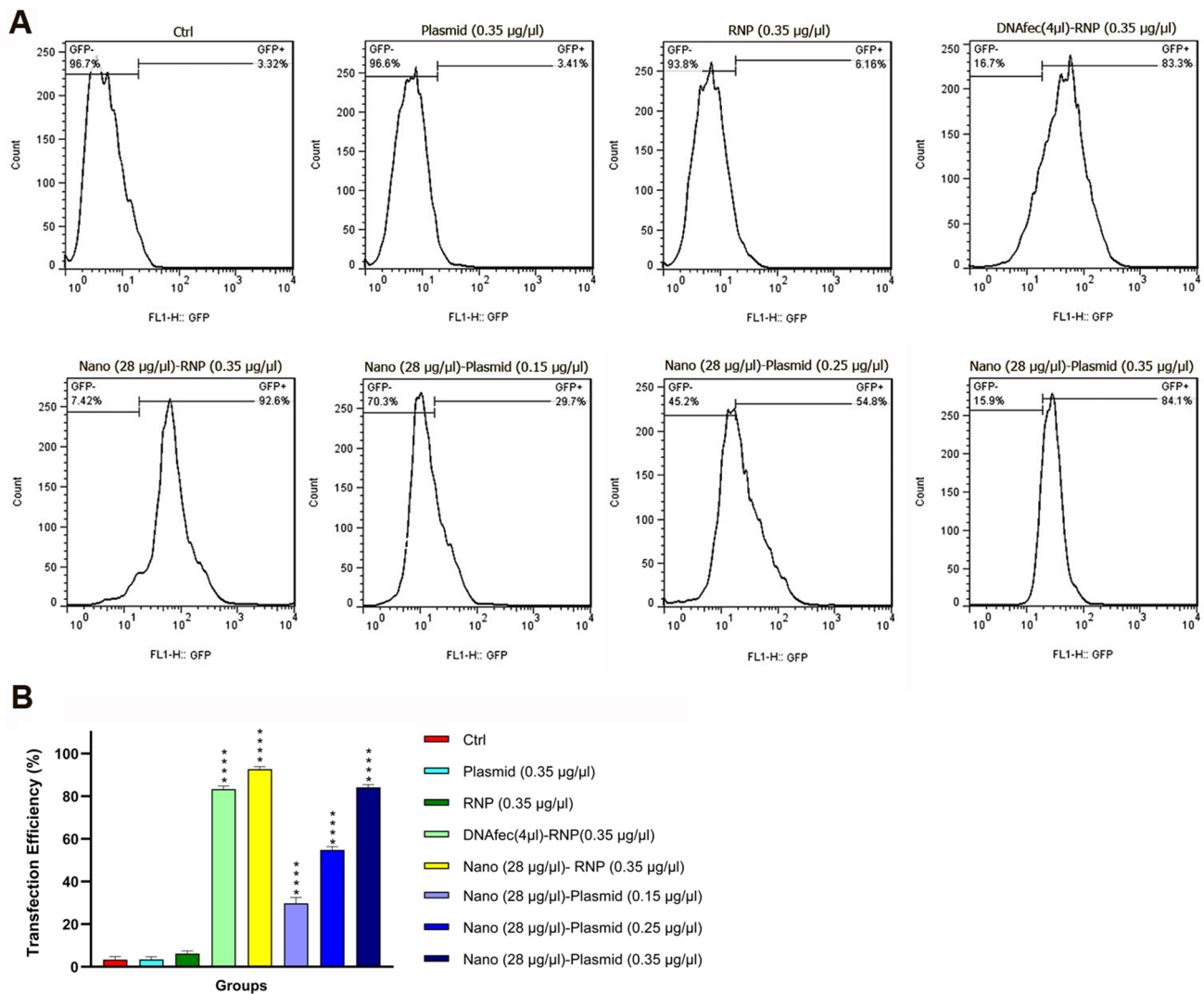
Fig. 9 Flow Cytometry analysis. A graphic illustration of flow cytometry analysis for all treated groups (**A**). Flow cytometry analysis showed delivery efficiency up to 84.1% for px458 plasmid and 92.6% for RNP complex by BSA-PEI NPs (**B**)
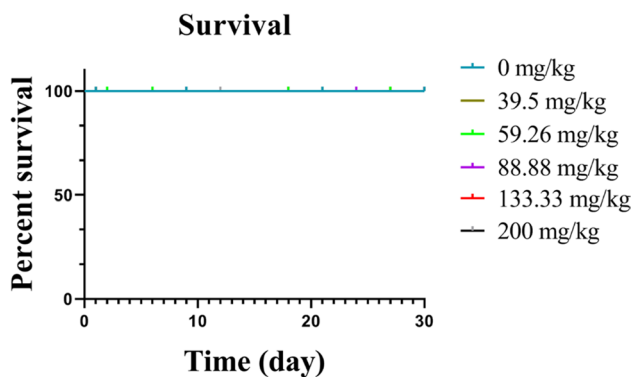

Fig. 10 In vivo biocompatibility assay. Selected concentrations (39.50, 59.26, 88.88, 133.33, and 200 mg/kg) of BSA-PEI NPs were injected to BALB/c mice via intravenous (IV) injection over a time period of 30 days. Percent survival of the animals over the time is shown on Y axis

Discussion

Safe and effective delivery of the CRISPR/Cas9 system is one of the necessities for CRISPR-based efficient genomic manipulation. However, employing CRISPR/Cas9 technology for genomic manipulations has been challenged by low delivery efficiency and potential toxicity of conventional delivery systems. In this study, we developed and evaluated PEI polymer-covered albumin nanoparticles for carrying CRISPR/Cas9 system components into MDA-MB-231 cells in plasmid and ribonucleoprotein forms. BSA was employed for the CRISPR/Cas9 delivery because of its unique biocompatibility properties and ease of synthesis. In this work, PEI was used to coat BSA NPs. PEI binds to the surface of BSA through electrostatic interactions. PEI coating was used with the aim of increasing cellular uptake by positively charging

the NPs surface as well as facilitating endosomal escape for successful delivery [36, 42, 43]. Several studies have shown that the use of PEI to coat NPs may ensure efficient delivery of CRISPR/Cas9 system components into desired cells. For example, Moradi et al. reported a novel nano-platform for the delivery of CRISPR/Cas9 plasmid form by integrating an arginine-disulfide linker with PEI. The resulted PEI-Arg nanoparticles improve plasmid releasing into cytoplasm while also enhancing membrane permeability and nuclear localization, resulting in an increased transfection efficiency. Another remarkable capability of these nanoparticles was the effective delivery of the CRISPR/Cas9 plasmid into local brain tissue [44]. Ryu et al. used branched PEI to deliver the CRISPR/Cas9 plasmid system into Neuro2a cells to target the Slc26a4 locus [36]. Interestingly, PEI forms compact complexes with gene materials and turns them into nanostructures, thus protecting the gene material against degradation. When the degree of branching and molecular weight of PEI increases, the capability of PEI to form complexes improves, therefore enhancing the efficiency of delivering materials; nevertheless, cytotoxic activity also increases dramatically with these factors. Moreover, it has been suggested that PEI at high ratios leads to a significant reduction in the viability of the cells and consequently reduces the delivery efficiency. However, at safe ratios, transfection efficiency improves and the CRISPR/Cas9 system is efficiently delivered into the cells [36]. In our work, combining BSA with PEI improved the safety and biocompatibility of formed BSA-PEI complex, demonstrating high transfection efficiency (up to $84.1 \pm 1.3\%$ for delivery of plasmid and $92.6 \pm 1.6\%$ for Cas9/sgRNA RNP). Cell viability is one of the major factors intrinsically associated with transfection efficiency. As the results of the MTT assay showed, MDA-MB-231 cells treated with a concentration of 28 μg/μl of BSA-PEI nanoparticles had no significant effect on cell viability. The concentration of 28 μg/μl of BSA-PEI NPs is the main concentration selected for the delivery of BSA-px458-PEI and BSA-RNP-PEI complexes into cells. Furthermore, the results of the in vivo biosafety assay revealed that BSA-PEI NPs are safe up to 200 mg/kg, therefore could be a suitable option for in vivo delivery. The "proton sponge" effect of the PEI polymer as well as the specific uptake of albumin protein by cancer cells are also likely to be the reasons for the high delivery efficiency of BSA-PEI NPs. Since cancer cells require more nutrients, they express high levels of Gp60 and SPARC (albumin receptors) on their surface, and can increase the cellular uptake of albumin NPs [45]. DLS and TEM were used to characterize the synthesized BSA-PEI NPs in this study. TEM image of BSA-PEI NPs showed spherical-shaped particles that are similar to the morphology of BSA NPs in different studies [46–49], confirming the correct synthesis of BSA-PEI NPs in our study. Additionally, the BSA-PEI NPs size obtained by TEM image analysis is

smaller than the size obtained by DLS, as expected. Since TEM allows the observation of NPs in a dry state, in which particles are in the most compact form.

Various studies have reported the high delivery efficiency of the CRISPR/Cas9 system employing nanomaterial-based delivery systems. For example, Chen et al. developed the liposome-templated hydrogel nanoparticles (LHNPs) for the delivery of Cas9/sgRNA RNP into U87 cells, flow cytometry analysis showed that LHNPs have an efficiency of 100% in the delivery of Cas9/sgRNA [50]. In another attempt, arginine-functionalized gold nanoparticles developed by Mout et al. delivered the Cas9/sgRNA RNP complex with an efficiency of 90% into target cells [51]. Polyethylene glycol phospholipid-modified cationic lipid nanoparticle (PLNP) developed by Zhang et al. to encapsulate and the delivery of Cas9/sgRNA into A375 cells showed 47% transfection efficiency [52]. In a study, human serum albumin nanoparticles (HSA) in complexing with stearyl polyethylenimine (stPEI) was employed to delivery of CRISPR/Cas9 plasmid into CT 26 cells. In this study, stPEI was complexed with plasmid as the core to form HSA (plasmid/stPEI/HSA) nanoparticles [45]. Besides high encapsulation ability and biocompatibility, the delivery system must be capable of overcoming physical and biological barriers, enabling for efficient and specific delivery of the CRISPR/Cas9 system into desired cells. In this regard, novel NIR-responsive biomimetic nanoparticles (UCNPs) were developed for CRISPR/Cas9 RNP delivery to achieve effective genome editing for HBV therapy. The UCNPs-CRISPR/Cas9 complexes were coated with cell-membrane-derived vesicles (CMs). The precise delivery of UCNPs-Cas9 into hepatocytes was obtained by using the principle of immune escape and the homotypic targeting potential of CMs [53]. Generally, bio-inspired nanomaterials, such as albumin-based nanoparticles, do not show an adverse interaction with serum and enable the safe and efficient release of cargo into the cell cytoplasm [54]. Our findings showed that, BSA-PEI NPs can also be a promising carrier to deliver CRISPR/Cas9 into other types of cells for gene editing in the future.

Conclusion

The CRISPR/Cas9 system has shown exceptional and efficient genome editing in several settings. However, scientists have been challenged to design and develop nanotechnology-based delivery systems in view of the importance of delivering the CRISPR/Cas9 system into cells efficiently and safely in order to implement effective genomic manipulations. The aim of the present study was to evaluate the efficiency of protein nanoparticles in the delivery of CRISPR/Cas9 system components in both plasmid and RNP forms. Due to its unique properties, BSA protein was carefully selected as

the protein-based carrier to deliver CRISPR/Cas9 system and was further modified by PEI polymer to improve cell penetration. Afterward, the synthesized BSA-PEI NPs were characterized in terms of biological and chemical structure properties. Based on our results, the synthesized NPs demonstrated high delivery of efficiency in delivering Cas9/sgRNA RNP and plasmid forms into the MDA-MB-231 cells. The attractive properties of BSA-PEI NPs in this study entail low cost, easy and convenient synthesis, high efficiency, good biocompatibility, and high loading capacity.

Declarations

Conflict of interest The authors declare no conflict of interest.

Ethical Approval This study was performed in accordance with the guidelines and standards of Research Ethics Committee under permission of Research Ethics Committees of Zanjan University of Medical (Ethical Code: IR.ZUMS.REC.1398.0141).

References

1. Liu, G., et al. (2021). The CRISPR-Cas toolbox and gene editing technologies. *Molecular Cell, 82*, 333–347.
2. Modell, A.E., et al., (2021) *CRISPR-based therapeutics: current challenges and future applications.* Trends in pharmacological sciences
3. Zhang, B. (2021). CRISPR/Cas gene therapy. *Journal of Cellular Physiology, 236*(4), 2459–2481.
4. Gaj, T. (2021). Next-generation CRISPR technologies and their applications in gene and cell therapy. *Trends in Biotechnology, 39*(7), 692–705.
5. Li, C., et al. (2021). CRISPR/Cas: A Nobel Prize award-winning precise genome editing technology for gene therapy and crop improvement. *Journal of Zhejiang University-Science B, 22*(4), 253–284.
6. Lee, H., & Sashital, D. G. (2022). Creating memories: molecular mechanisms of CRISPR adaptation. *Trends in Biochemical Sciences, 47*, 467–476.
7. K Bhushan 2020 Evolution and molecular mechanism of CRISPR/Cas9 systems genome engineering via CRISPR-Cas9 System Elsevier 15 25
8. Jinek, M., et al. (2012). A programmable dual-RNA–guided DNA endonuclease in adaptive bacterial immunity. *Science, 337*(6096), 816–821.
9. Jiang, F., & Doudna, J. A. (2017). CRISPR–Cas9 structures and mechanisms. *Annual Review of Biophysics, 46*, 505–529.
10. Lan, T., et al. (2022). Genome editing via non-viral delivery platforms: Current progress in personalized cancer therapy. *Molecular Cancer, 21*(1), 1–15.
11. Ho, D., et al. (2020). Enabling technologies for personalized and precision medicine. *Trends in Biotechnology, 38*(5), 497–518.
12. Rahimi, H., et al. (2021). CRISPR systems for COVID-19 diagnosis. *ACS Sensors, 6*(4), 1430–1445.
13. Uyhazi, K.E. and J. Bennett, A CRISPR view of the. (2020). Nobel prize in chemistry. *The Journal of Clinical Investigation*. https://doi.org/10.1172/JCI145214
14. Rahimi, H., et al. (2020). Harnessing nanoparticles for the efficient delivery of the CRISPR/Cas9 system. *Nano Today, 34*, 100895.
15. Taha, E. A., Lee, J., & Hotta, A. (2022). Delivery of CRISPR-Cas tools for in vivo genome editing therapy: Trends and challenges. *Journal of Controlled Release, 342*, 345.
16. Song, X., et al. (2021). Delivery of CRISPR/Cas systems for cancer gene therapy and immunotherapy. *Advanced drug delivery reviews, 168*, 158–180.
17. Challa, A. K., et al. (2021). Validation of gene editing efficiency with CRISPR-Cas9 system directly in rat zygotes using electroporation mediated delivery and embryo culture. *MethodsX, 8*, 101419.
18. Abe, T., et al. (2020). Pronuclear microinjection during S-phase increases the efficiency of CRISPR-Cas9-assisted knockin of large DNA donors in mouse zygotes. *Cell Reports, 31*(7), 107653.
19. Lee, S., Kim, Y.-Y., & Ahn, H. J. (2021). Systemic delivery of CRISPR/Cas9 to hepatic tumors for cancer treatment using altered tropism of lentiviral vector. *Biomaterials, 272*, 120793.
20. Gao, J., et al. (2019). Viral vector-based delivery of CRISPR/Cas9 and donor DNA for homology-directed repair in an in vitro model for canine hemophilia B. *Molecular Therapy-Nucleic Acids, 14*, 364–376.
21. Mizuno, N., et al. (2018). Intra-embryo gene cassette knockin by CRISPR/Cas9-mediated genome editing with adeno-associated viral vector. *Iscience, 9*, 286–297.
22. Yang, P., et al. (2022). Nano-vectors for CRISPR/Cas9-mediated genome editing. *Nano Today, 44*, 101482.
23. Li, Q., et al. (2022). Co-delivery of doxorubicin and CRISPR/Cas9 or RNAi-expressing plasmid by chitosan-based nanoparticle for cancer therapy. *Carbohydrate Polymers, 287*, 119315.
24. Yu, M., et al. (2021). Latest progress in the study of nanoparticle-based delivery of the CRISPR/Cas9 system. *Methods, 194*, 48–55.
25. Zhang, X., et al. (2022). Robust genome editing in adult vascular endothelium by nanoparticle delivery of CRISPR-Cas9 plasmid DNA. *Cell reports, 38*(1), 110196.
26. Shin, H., & Kim, J. (2022). Nanoparticle-based non-viral CRISPR delivery for enhanced immunotherapy. *Chemical Communications, 58*, 1860–1870.
27. Francis, C., et al. (2022). Systemic biodistribution and hepatocyte-specific gene editing with CRISPR/Cas9 using hyaluronic acid-based nanoparticles. *Nanomedicine Nanotechnology, Biology and Medicine, 40*, 102488.
28. Wang, Y., et al. (2021). In vivo targeted delivery of nucleic acids and CRISPR genome editors enabled by GSH-responsive silica nanoparticles. *Journal of Controlled Release, 336*, 296–309.
29. Li, X., et al. (2021). Enhancing gene editing efficiency for cells by CRISPR/Cas9 system-loaded multilayered nanoparticles assembled via microfluidics. *Chinese Journal of Chemical Engineering, 38*, 216–220.
30. Phan, Q. A., et al. (2022). CRISPR/Cas-powered nanobiosensors for diagnostics. *Biosensors and Bioelectronics, 197*, 113732.
31. Gharbavi, M., et al. (2020). Cholesterol-conjugated bovine serum albumin nanoparticles as a tamoxifen tumor-targeted delivery system. *Cell Biology International, 44*(12), 2485–2498.

32. Cruz, L. J., et al. (2021). PLGA-nanoparticles for intracellular delivery of the CRISPR-complex to elevate fetal globin expression in erythroid cells. *Biomaterials, 268*, 120580.

33. Rui, Y., et al. (2020). Poly (beta-amino ester) nanoparticles enable nonviral delivery of CRISPR-Cas9 plasmids for gene knockout and gene deletion. *Molecular Therapy-Nucleic Acids, 20*, 661–672.

34. González-Domínguez, I., et al. (2022). Micrometric DNA/PEI polyplexes correlate with higher transient gene expression yields in HEK 293 cells. *New Biotechnology, 68*, 87–96.

35. Sabin, J., et al. (2022). New insights on the mechanism of polyethylenimine transfection and their implications on gene therapy and DNA vaccines. *Colloids and Surfaces B: Biointerfaces, 210*, 112219.

36. Ryu, N., et al. (2018). Effective PEI-mediated delivery of CRISPR-Cas9 complex for targeted gene therapy. *Nanomedicine: Nanotechnology, Biology and Medicine, 14*(7), 2095–2102.

37. Zhang, C., et al. (2010). Targeted minicircle DNA delivery using folate–poly (ethylene glycol)–polyethylenimine as nonviral carrier. *Biomaterials, 31*(23), 6075–6086.

38. Benjaminsen, R. V., et al. (2013). The possible "proton sponge" effect of polyethylenimine (PEI) does not include change in lysosomal pH. *Molecular Therapy, 21*(1), 149–157.

39. Zakeri, A., et al. (2018). Polyethylenimine-based nanocarriers in co-delivery of drug and gene: A developing horizon. *Nano Reviews & Experiments, 9*(1), 1488497.

40. Zaboli, K.A., et al., (2022) *Plasmid-based CRISPR-Cas9 system efficacy for introducing targeted mutations in CD81 gene of MDA-MB-231 cell line*. Folia Histochemica et Cytobiologica

41. Neun, B. W., Ilinskaya, A. N., & Dobrovolskaia, M. A. (2018). Updated method for in vitro analysis of nanoparticle hemolytic properties. *Characterization of nanoparticles intended for drug delivery* (pp. 91–102). Springer.

42. Boussif, O., et al. (1995). A versatile vector for gene and oligonucleotide transfer into cells in culture and in vivo: Polyethylenimine. *Proceedings of the National Academy of Sciences, 92*(16), 7297–7301.

43. Di Gioia, S., & Conese, M. (2008). Polyethylenimine-mediated gene delivery to the lung and therapeutic applications. *Drug Design, Development and Therapy, 2*, 163.

44. Moradi, P., et al. (2021). Smart arginine-equipped polycationic nanoparticles for p/CRISPR delivery into cells. *Nanotechnology, 33*(7), 075104.

45. Cheng, W.-J., et al. (2018). Stearyl polyethylenimine complexed with plasmids as the core of human serum albumin nanoparticles noncovalently bound to CRISPR/Cas9 plasmids or siRNA for disrupting or silencing PD-L1 expression for immunotherapy. *International Journal of Nanomedicine, 13*, 7079.

46. Mohammadhassan, Z., et al. (2022). Preparation of copper oxide nanoparticles coated with bovine serum albumin for delivery of methotrexate. *Journal of Drug Delivery Science and Technology, 67*, 103015.

47. Siri, M., et al. (2019). Effect of structure in ionised albumin based nanoparticle: Characterisation, Emodin interaction, and in vitro cytotoxicity. *Materials Science and Engineering: C, 103*, 109813.

48. Tarhini, M., et al. (2018). Protein-based nanoparticle preparation via nanoprecipitation method. *Materials, 11*(3), 394.

49. Bali, G., et al. (2018). Preparation, physico-chemical characterization and pharmacodynamics of ceftriaxone loaded BSA nanoparticles. *Nanomed Nanotech J, 9*(34), 1–6.

50. Chen, Z., et al. (2017). Targeted delivery of CRISPR/Cas9-mediated cancer gene therapy via liposome-templated hydrogel nanoparticles. *Advanced functional materials, 27*(46), 1703036.

51. Mout, R., et al. (2017). Direct cytosolic delivery of CRISPR/Cas9-ribonucleoprotein for efficient gene editing. *ACS Nano, 11*(3), 2452–2458.

52. Zhang, L., et al. (2017). Lipid nanoparticle-mediated efficient delivery of CRISPR/Cas9 for tumor therapy. *NPG Asia Materials, 9*(10), e441–e441.

53. Wang, D., et al. (2022). CRISPR/Cas9 delivery by NIR-responsive biomimetic nanoparticles for targeted HBV therapy. *Journal of nanobiotechnology, 20*(1), 1–16.

54. Prajapati, R., & Somoza, Á. (2021). Albumin nanostructures for nucleic acid delivery in cancer: Current trend, emerging issues, and possible solutions. *Cancers, 13*(14), 3454.

Authors and Affiliations

Hossein Rahimi[1] · Kasra Arbabi Zaboli[1] · Jose Thekkiniath[2] · Seyed Hossein Mousavi[3] · Behrooz Johari[1,8] · Mohammad Reza Hashemi[4] · Hamed Nosrati[5] · David Goldschneider[6] · Agnes Bernet[7] · Hossein Danafar[5] · Saeed Kaboli[1,8]

Hossein Rahimi
hrahimi1995@yahoo.com

Kasra Arbabi Zaboli
kasra.arbabi@gmail.com

Jose Thekkiniath
jose.thekkiniath@fullerlabs.net

Seyed Hossein Mousavi
mousavi_1887@yahoo.com

Behrooz Johari
dr.johari@zums.ac.ir

Mohammad Reza Hashemi
m.hashemi1369@ut.ac.ir

Hamed Nosrati
nosrati.hamed2020@gmail.com

David Goldschneider
davidgoldschneider@netrispharma.com

Agnes Bernet
agnes.bernet@lyon.unicancer.fr

1   Department of Medical Biotechnology, School of Medicine, Zanjan University of Medical Sciences, Zanjan, Iran

2   Fuller Laboratories, 1312 East Valencia Drive, Fullerton, CA 92831, USA

3   Molecular Bank, Iranian Biological Resource Center, ACECR, Karaj, Iran

4   Department of Animal Sciences, School of Agriculture, Tehran University, Karaj, Iran

5   Zanjan Pharmaceutical Biotechnology Research Center, Zanjan University of Medical Sciences, Zanjan, Iran

6   Netris Pharma, 69008 Lyon, France

7   Apoptosis, Cancer and Development Laboratory - Equipe Labellisée 'La Ligue', LabEX DEVweCAN, Institut Convergence Plascan, Centre de Cancérologie de Lyon, INSERM U1052-CNRS UMR5286, Université de Lyon, Université Claude Bernard Lyon1, Centre Léon Bérard, Lyon, France

8   Cancer Gene Therapy Research Center, Zanjan University of Medical Sciences, Zanjan, Iran